iScience, Volume *24*

Supplemental information

Immunogenic tumor cell death promotes dendritic cell migration and inhibits tumor growth via enhanced T cell immunity

Taiki Moriya, Kurumi Kitagawa, Yuuki Hayakawa, Hiroaki Hemmi, Tsuneyasu Kaisho, Satoshi Ueha, Ryoyo Ikebuchi, Ippei Yasuda, Yasutaka Nakanishi, Tetsuya Honda, Koji Matsushima, Kenji Kabashima, Mizuki Ueda, Yutaka Kusumoto, Tatyana Chtanova, and Michio Tomura

Figure S1; related to Figure 1
DT-induced cell death enhances expression and release of DAMPs molecules.

Figure S2; related to Figure 1
Gating strategies for cells in tumors.

Figure S3; related to Figure 2
Analysis of dynamics of tumor infiltrating myeloid cells in MC38-TfROVA-DTRs inoculated KikGR mice.

Figure S4; related to Figure 3
Gating strategy and proportions of migratory DC subsets in dLNs.

Figure S5; related to Figure 3
Immunogenic tumor cell death enhances Ti-DC migration to dLNs.

Figure S6; related to Figure 4
Enhanced Ti-DC migration induced by immunogenic tumor cell death is inhibited by blocking of ATP-P2X7R, HMGB1-TLR4, and G*ai* signaling and S1P-S1PR1 pathways.

Figure S7; related to Figure 6
Tumor cell death induction does not increase expression levels of CD80, CD86, and H-2K^{b} on KikGR-Red CD103^{+} Ti-DCs in dLNs.

Figure S8; related to Figure 7

Table S1; related to Methods
Antibodies for Flow cytometry

Transparent Methods

Supplemental References

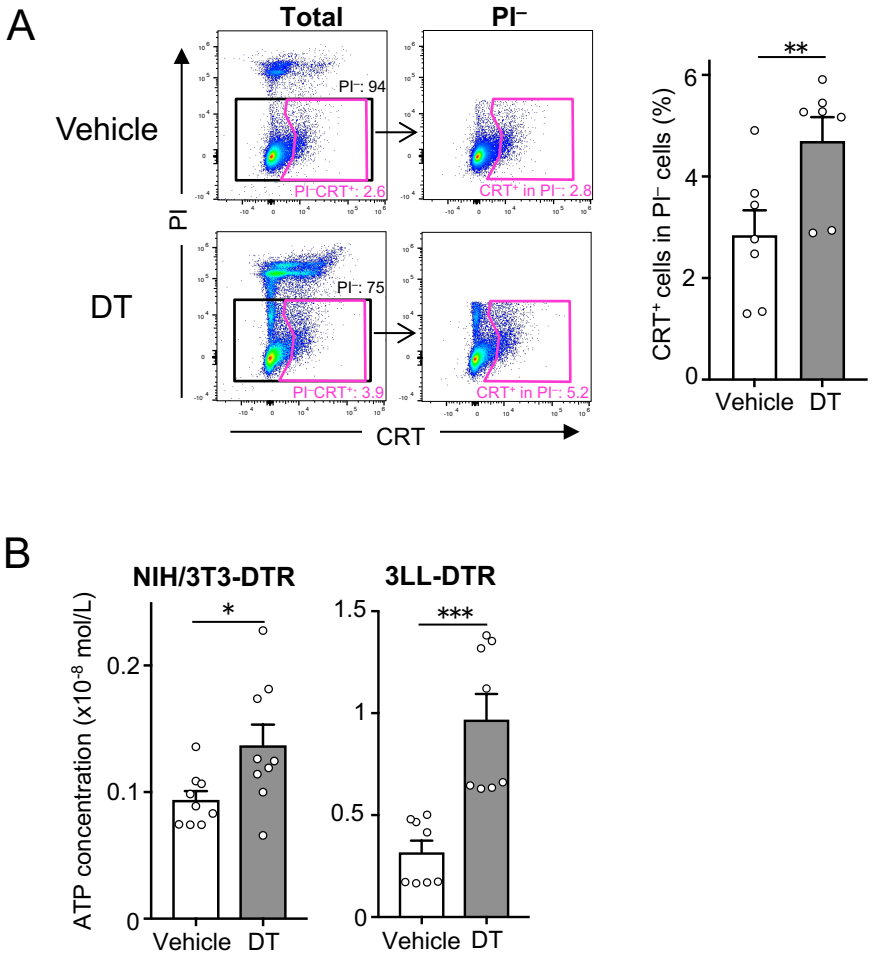

Figure S1; related to Figure 1
DT-induced cell death enhances expression and release of DAMPs molecules.
(A) MC38/TfROVA-DTRs cells 18 hours after vehicle or DT treatment. Gating strategy (left) and proportion (right) of CRT^+ cells in PI^- cell. Numbers in dot plots indicate frequencies of gated population (%) of parent population. Bar graph shows means ± SEM of pooled data from two independent experiments (n=7). $^{**}p<0.01$ (Mann-Whitney U test). (B) ATP concentration in culture supplement of NIH/3T3-DTR and 3LL-DTR cells 12 hours after vehicle or DT treatment. Bar graphs show means ± SEM of pooled data from two independent experiments (n=9). $^{*}P<0.05$, $^{***}p<0.001$ (Mann-Whitney U test).

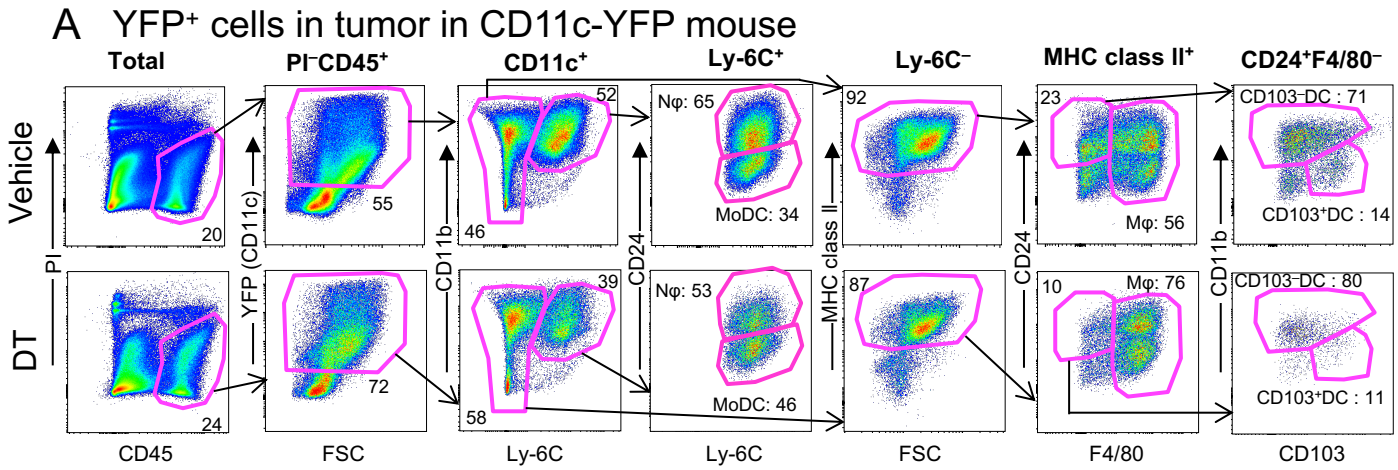

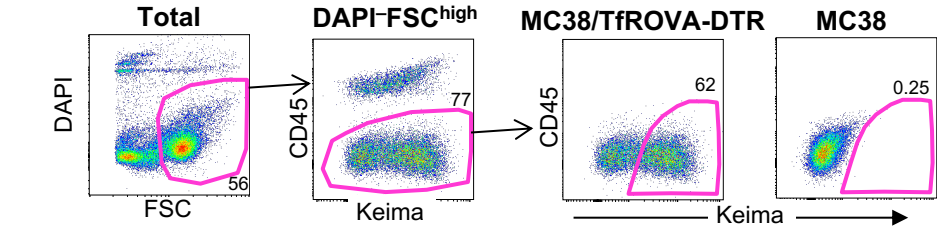

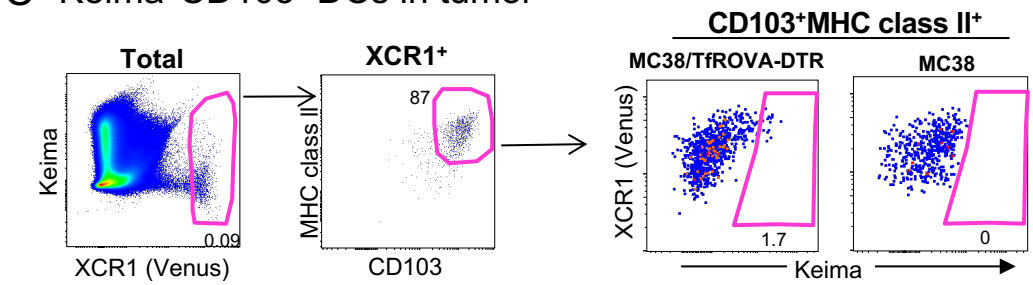

Figure S2; related to Figure 1
Gating strategies for cells in tumors.
(A) Gating strategy for analysis of YFP$^+$ cells in MC38-TfROVA-DTR tumors in CD11c-YFP mice 24 hours after vehicle or DT treatment. (B) Gating strategy for Keima$^+$ live tumor cells in MC38-TfROVA-DTR cells (left) and MC38 cells (right) inoculated mice. (C) Gating strategy for Keima$^+$ Venus$^+$ CD103$^+$ DCs in MC38-TfROVA-DTR cells (left) and MC38 cells (right) inoculated XCR1-Venus mice. Numbers in dot plots indicate frequencies of gated population (%) of parent population.

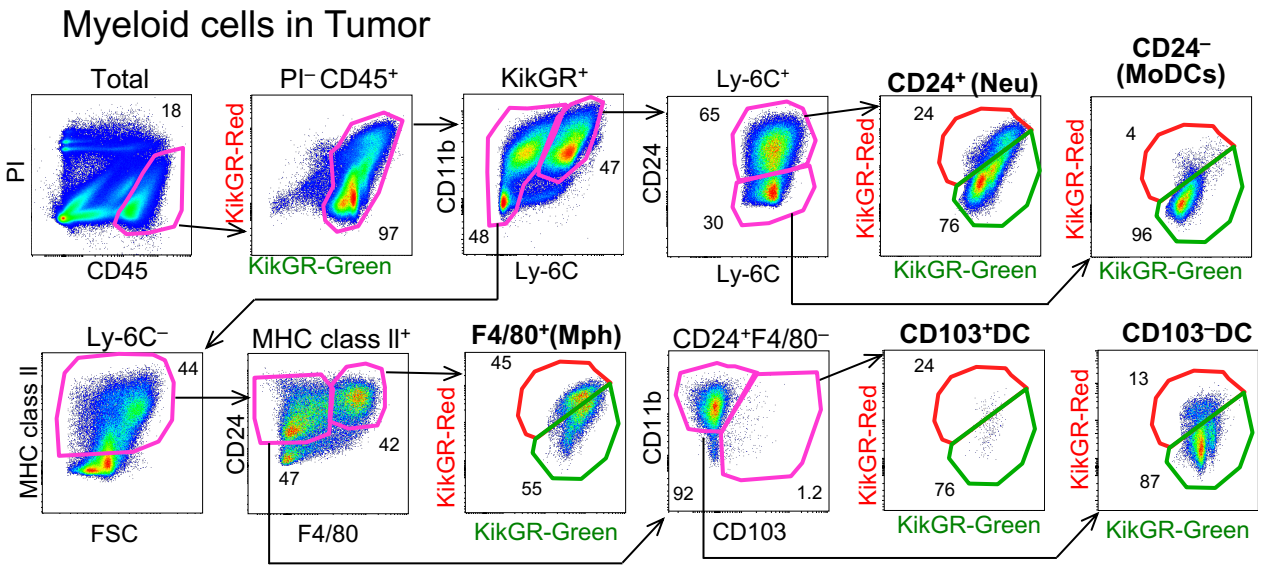

Figure S3; related to Figure 2
Analysis of dynamics of tumor infiltrating myeloid cells in MC38-TfROVA-DTRs inoculated KikGR mice.
Gating strategy for myeloid cells in MC38-TfROVA-DTR tumors inoculated in KikGR mice and photoconverted 24 hours prior to analysis. Numbers in dot plots indicate frequencies of gated population as a % of parent population.

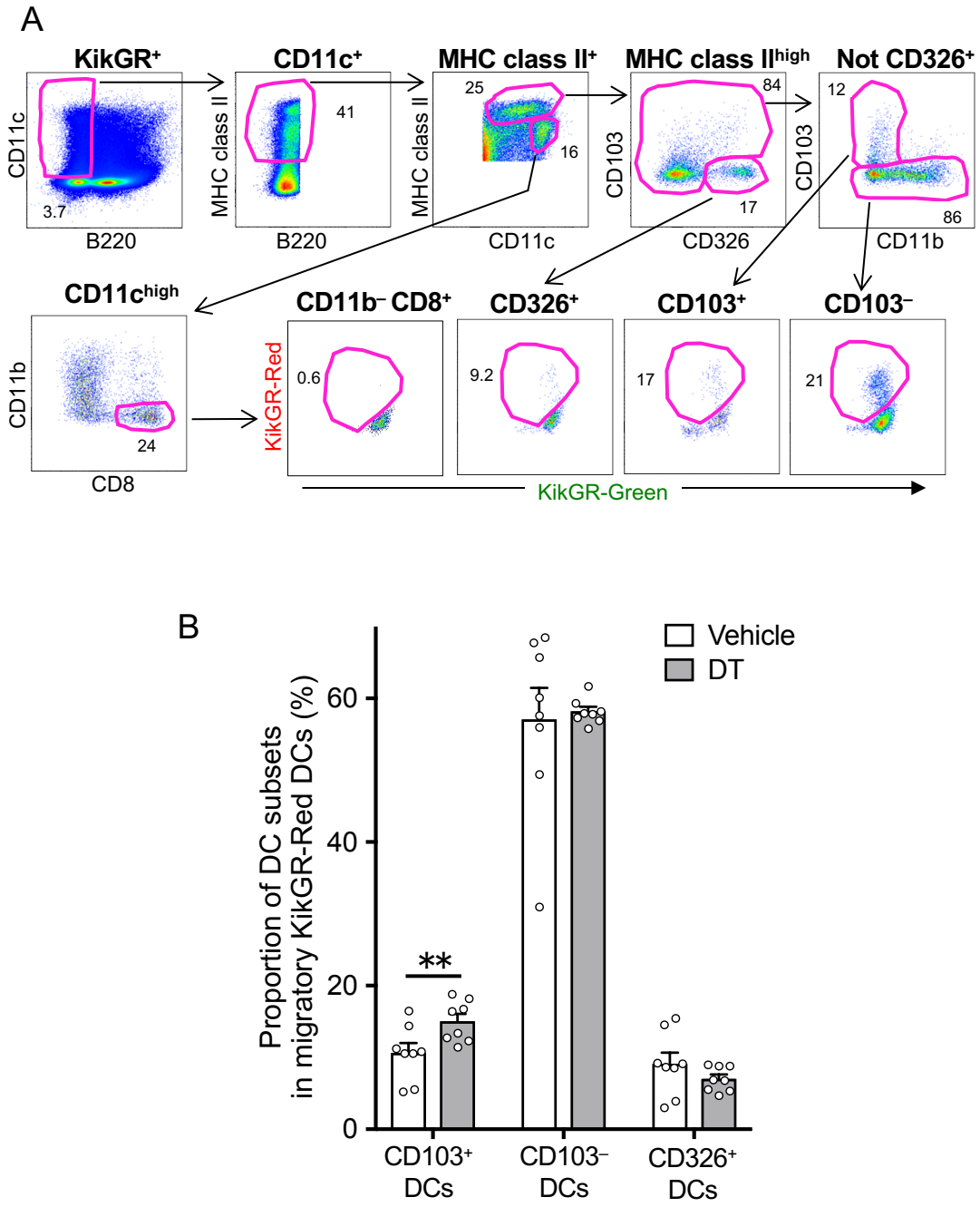

Figure S4; related to Figure 3
Gating strategy and proportions of migratory DC subsets in dLNs
(A) Gating strategy for DCs in dLNs of MC38-TfROVA-DTR tumors inoculated in KikGR mice 24 hours following photoconversion of tumors. Numbers in dot plots indicate frequencies of gated population (%) of parent population. (B) Proportion of 3 DC subsets in migratory KikGR-Red DCs (%) in dLNs in vehicle or DT treated KikGR mice 24 hours after photoconversion. Bar graph shows means ± SEM of pooled data from four independent experiments (n=8). ** P<0.01, (Mann-Whitney U test).

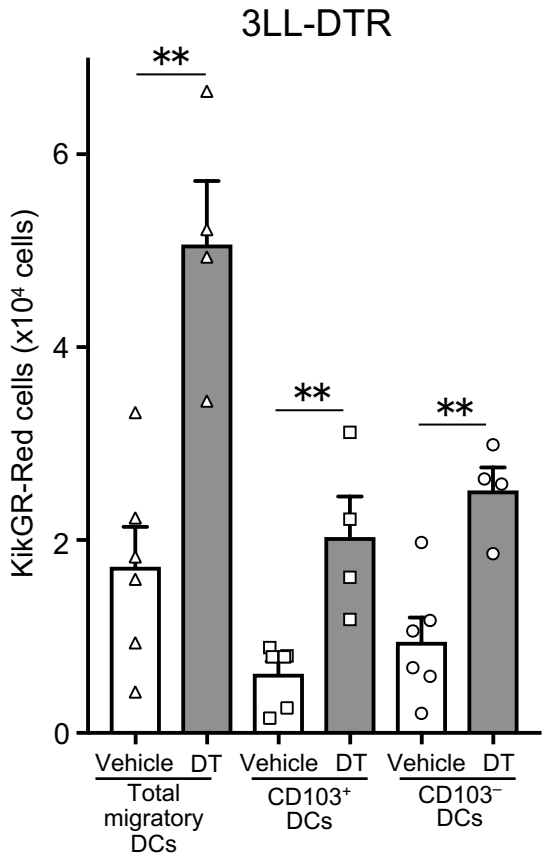

Figure S5; related to Figure 3
Immunogenic tumor cell death enhances Ti-DC migration to dLNs.
KikGR-Red cells in 3 DC subsets in dLNs 24 hours following photoconversion of tumors and vehicle or DT-treated 3LL-DTR tumor in KikGR mice. Bar graphs show means ± SEM of pooled data from two independent experiments (n=4-6). ** P<0.01, (Mann-Whitney U test).

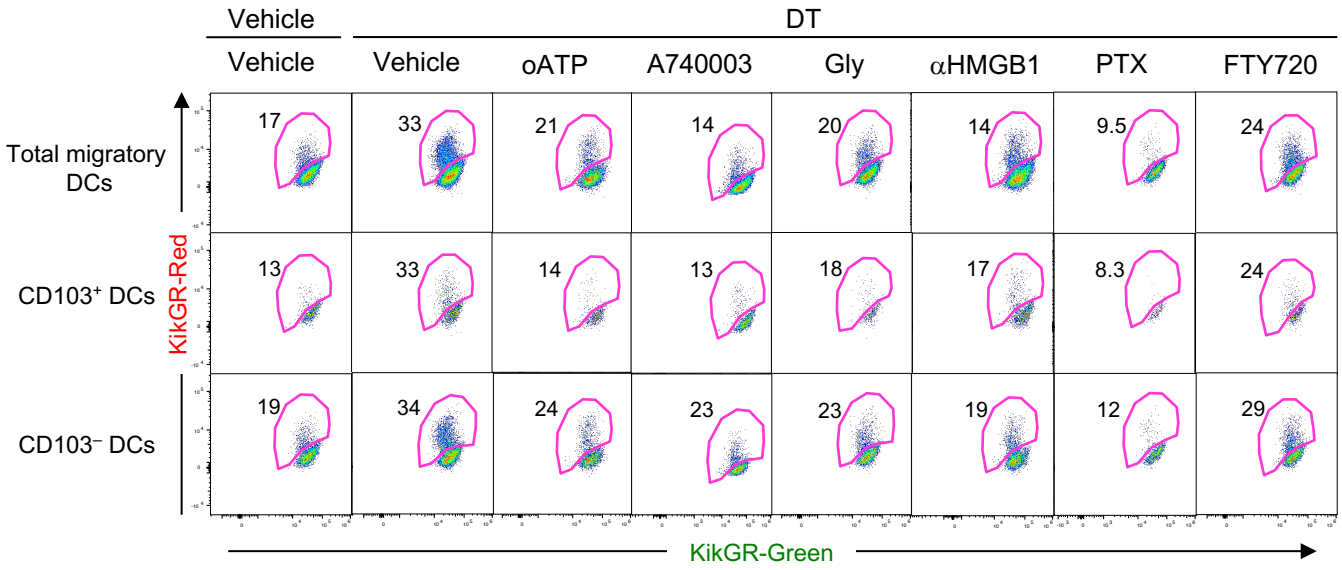

Figure S6; related to Figure 4
Enhanced Ti-DC migration induced by immunogenic tumor cell death is inhibited by blocking of ATP-P2X7R, HMGB1-TLR4, and G*αi* signaling and S1P-S1PR1 pathways.
Representative flow cytometry plots of total migratory DCs, $CD103^+$ DCs, and $CD103^-$ DCs in dLNs of MC38-TfROVA-DTR tumors inoculated in KikGR mice analyzed 24 hours following photoconversion of tumors and indicated treatments. Numbers in dot plots indicate frequencies of gated population (%) of parent population. Data are representative of two to four independent experiments.

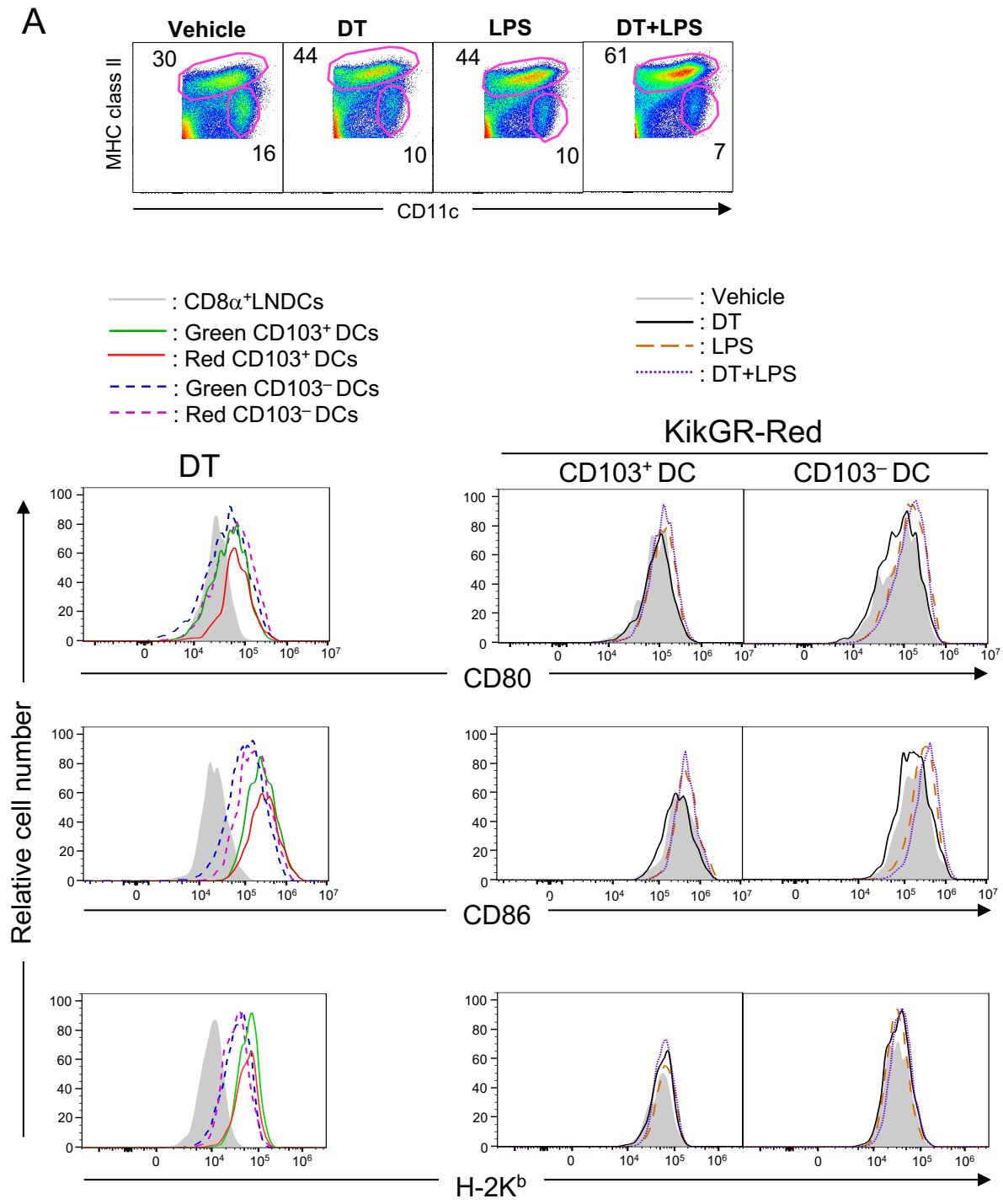
A
Vehicle
DT
LPS
DT+LPS
MHC class II
30
16
44
10
44
10
61
7
CD11c
B
: CD8α+LNDCs
: Green CD103+ DCs
: Red CD103+ DCs
: Green CD103− DCs
: Red CD103− DCs
: Vehicle
: DT
: LPS
: DT+LPS
KikGR-Red
DT
CD103+ DC
CD103− DC
Relative cell number
CD80
CD86
H-2Kb

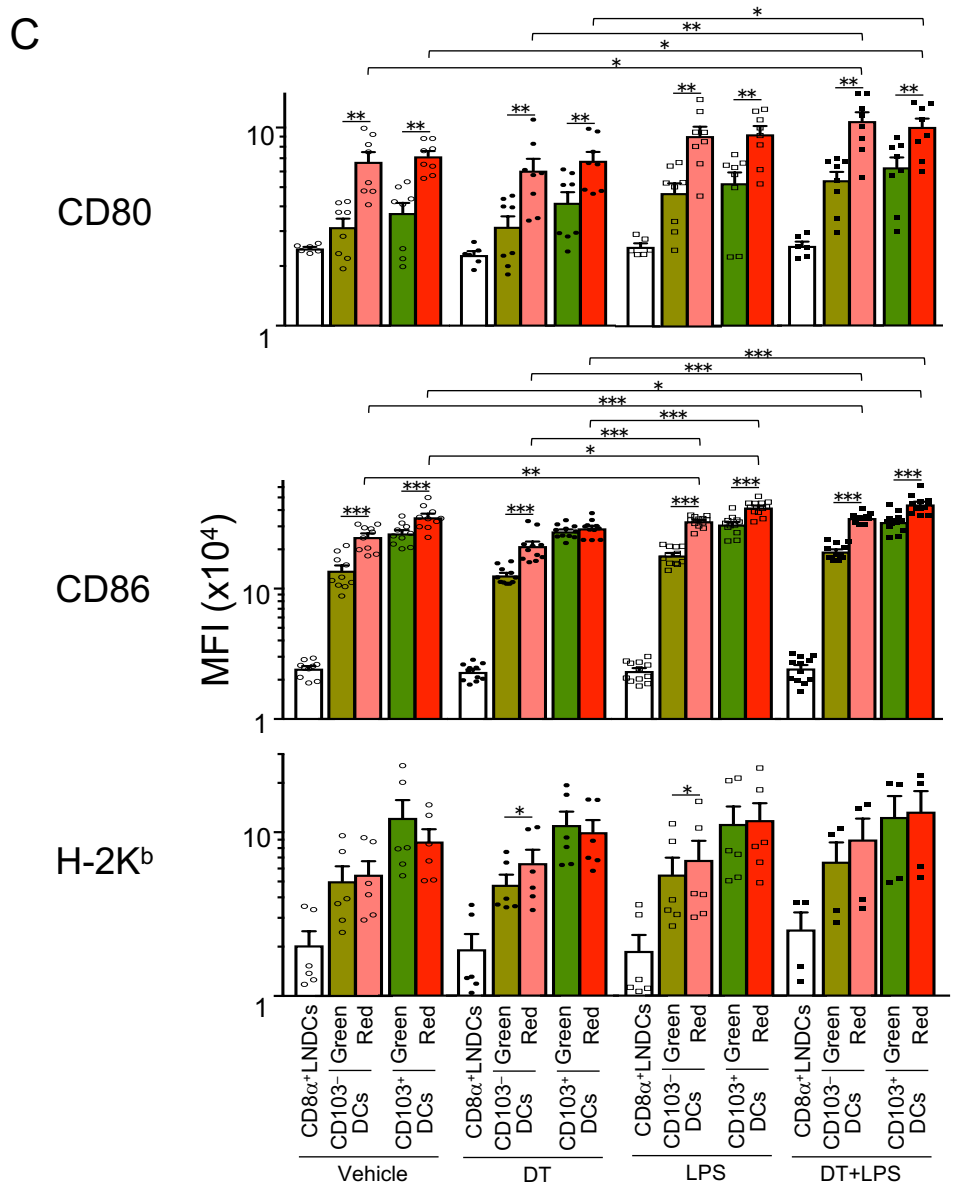

Figure S7; related to Figure 6
Tumor cell death induction does not increase expression levels of CD80, CD86, and H-2K^b on KikGR-Red CD103$^+$ Ti-DCs in dLNs.
(A) Representative flow cytometry plots of migratory DCs and LNDCs in dLN of tumor bearing KikGR mice 24 hours following photoconversion of tumors and vehicle, DT and/or LPS treatments. Numbers in dot plots indicate frequencies of gated population (%) of parent population. Data are representative of at least nine independent experiments. (B) Representative histogram plots of CD80, CD86, and H-2K^b expression in CD8α$^+$ LNDC, KikGR-Green and KikGR-Red CD103$^+$ and CD103$^-$ DCs in dLNs from DT treated KikGR mice bearing tumors consisting of MC38-TfROVA-DTR and MC38 cells (3:7 ratio) 24 hours after photoconversion (left) and in KikGR-Red CD103$^+$ and CD103$^-$ DCs in dLNs from vehicle, DT and/or LPS treated KikGR mice 24 hours after photoconversion (right). Data are representative of at least two independent experiments. (C) MFI values for CD80, CD86 and H-2K^b in each DC subset. Bar graphs show means ± SEM of pooled data from at least two independent experiments (n=4-11). Statistical comparisons were performed using Wilcoxon matched-pairs signed rank test (comparison between KikGR-Green and KikGR-Red cells in each DC subset, *$p < 0.05$, **$p < 0.01$, ***$p < 0.001$) or one-way ANOVA with Kruskal-Wallis test with Dunn's comparisons test (comparison among 4 treatments for the same DC subset, *$p < 0.05$, **$p < 0.01$, ***$p < 0.001$).

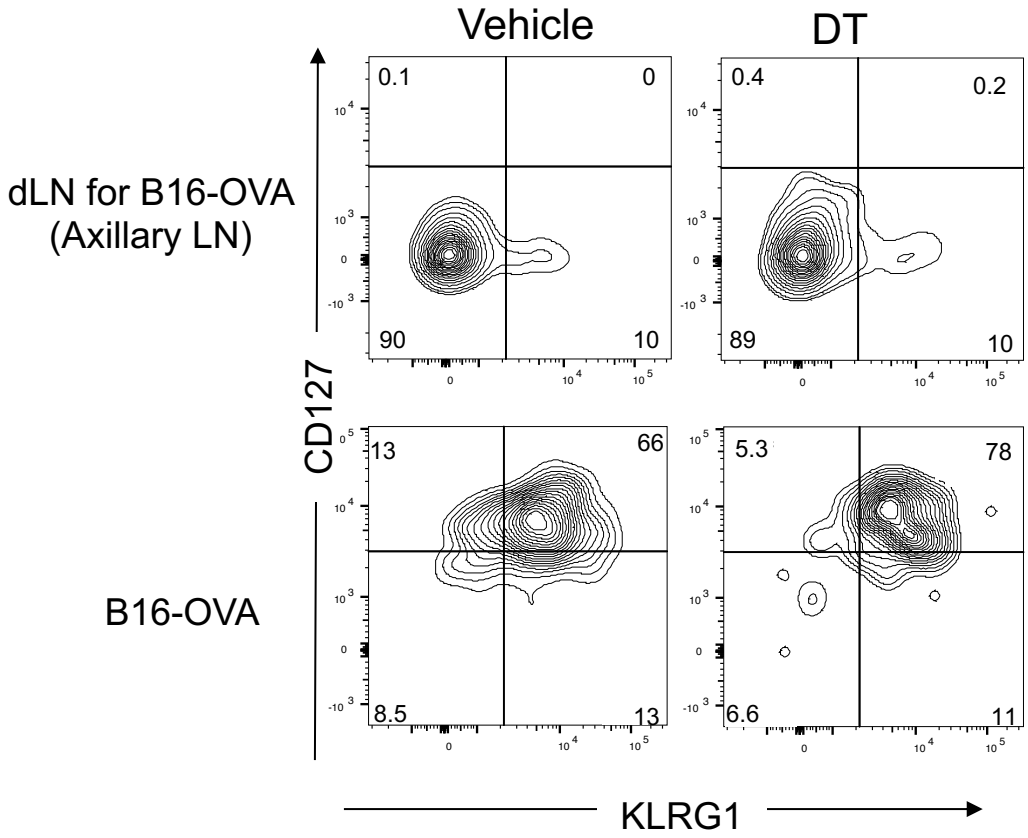

Figure S8; related to Figure 7
Representative flow cytometry plots of OVA-specific $CD8^+$ T cells in dLNs for B16-OVA from vehicle or DT treated tumor bearing mice 2 days after tumor cell death induction. Data are representative of two independent experiments.

Table S1; related to Methods
Antibodies for flow cytometry

Antibody	Clone
CD4	RM4-5
CD5	53-7.3
CD8α	53-6.7
CD11b	M1/70
CD11c	N418
CD19	6D5
CD24	M1/69
CD44	1M7
CD45	30-F11
CD45R/B220	RA3-6B2
CD45.1	A20
CD45.2	104
CD49b/Pan-NK cells	DX5
CD62L	MEL-14
CD69	H1.2F3
CD80	16-10A1
CD86	GL1
CD90.2	53-2.1
CD103	2E7
CD107a	1D4B
CD127	A7R34
CD197 (CCR7)	4B12
CD279 (PD1)	RMP1-30
CD326	G8.8
I-A/I-E	M5/114. 15. 2
H-2K^{b}	AF6-88.5
F4/80	BM8
Ly-6C	HK1.4
TER-119	TER-119
Calreticulin	EPR3924
KLRG1	2F1/KLRG1
TCR-Vα2	B20.1

Transparent Methods

Mice

Knock-in mice carrying KikGR cDNA under the CAG promoter (KikGR mice) were made previously (Tomura et al., 2014). XCR1-DTR mice and XCR1-Venus mice were generated as described previously (Yamazaki et al., 2013). CD11c-YFP mice were kindly provided by Prof. Michel C. Nussenzweig (Lindquist et al., 2004). OT-I transgenic mice (Tg) expressing a TCR specific for OVA in the context of H-2K^{b} (Hogquist et al., 1994) were obtained from Taconic Inc. C57BL/6 mice were purchased from Japan SLC Inc. These mice were bred in specific pathogen–free facilities at Osaka Ohtani University. All experimental procedures were approved by the Institutional Animal Care and Use Committee of Osaka-Ohtani University Faculty of Pharmacy.

Cell lines

The colon adenocarcinoma cell line MC38 (Spiess et al., 1987) was obtained from Shunsuke Chikuma (Kyoto University). The fragment encoding Nuc-tdKeima with NheI and SphI sites was cloned from the pdKeima-NLS3/MC1 vector (Kogure et al., 2006), kind gift from Atsushi Miyawaki (Brain Science Institute, RIKEN). The fragment encoding IRES2 with SphI and BstXI sites was cloned from CSII-CMV-MCS-IRES2-Venus vector kindly provided by Dr Hiroyuki Miyoshi (BioResource center, RIKEN). The TfROVA fragment encoding a fusion protein consisting of the transmembrane domain of the transferrin receptor and OVA (149-385) with BstXI and XbaI sites was cloned from the pIRES puro2-TfrOVA vector (Teasdale et al., 1992). The fragments encoding Nuc-tdKeima with NheI and SphI sites, IRES2 with SphI and BstXI sites, and TfROVA with BstXI and XbaI sites were ligated and cloned into the NheI and XbaI digestion site of CSII-CMV-MCS-IRES2-Venus by blunt end ligation (CSII-CMV-Nuc-tdKeima-IRES2-TfROVA). pTRECK6 and pCAGTR6-GFP was kindly provided by Dr. Kenji Kohno (Nara Institute of Science and Technology)(Furukawa et al., 2006; Saito et al., 2001). The fragment of human HB-EGF (DTR) complementary DNA (cDNA) was isolated from pTRECK6 by EcoRI digestion, and cloned into EcoRI site of pCAGTR6-GFP, and the fragment of CAG-HB-EGF was isolated by SalI and HindIII digestion. pBS-Lox-PGK-gb2-Hyg-Lox sequence was isolated from pBS-Lox-PGK-gb2-Hyg-Lox vector (Gene Bridges) by NotI and XhoI

digestion, and cloned into the same digestion site in pBluescript II-SK+ vector, and then the fragment of CAG-HB-EGF was cloned into SalI and HindIII digestion site, and fragment of pBS-Lox-Hyg-CAG-HB-EGF was obtained by XhoI and NotI digestion. CSII-CMV-Nuc-tdKeima-IRES2-TfROVA vector was digested by SacII, and XhoI and NotI digestion sites were introduced in SacII digestion site of CSII- CMV-Nuc-tdKeima-IRES2-TfROVA by using synthetic oligomers CSII-S: CTGTATCAAGCACATCGCAACCAACGCCG and CSII-AS: AGCAGGCCGCGGGCGGCCGCTTCAGTTC. And then, obtained vector was digested by XhoI and NotI and the fragment of pBS-Lox-Hyg-CAG-HB-EGF was cloned (pCSII-CMV-Nuc-tdKeima-IRES2-TfrOVA-Lox-PGK-Hyg-Lox-CAG-HB-EGF). To obtain MC38/TfROVA-DTRs and MC38/TfROVA, linearized pCSII-CMV-Nuc-tdKeima-IRES2-TfrOVA-Lox-PGK-Hyg-Lox-CAG-HB-EGF or pCSII- CMV-Nuc-tdKeima-IRES2-TfROVA was transfected to MC38 with Amaxa (Lonza), and transfectants were selected by zeocin, respectively and Keima^{+} cells were sorted and used for experiments. B16-OVA was kindly gifted by Dr. Masakazu Hattori (Kyoto University). pCAGTR6-GFP was transfected into 3LL and NIH/3T3 using Lipofectamine 3000 (Thermo Fisher Scientific K. K.) to establish 3LL and NIH/3T3 expressing DTR (3LL-DTR, NIH/3T3-DTR). MC38, B16, 3LL-DTR, NIH/3T3-DTR, MC38/TfROVA-DTR and B16-OVA cell lines were maintained in culture medium consisted of Roswell Park Memorial Institute-1640 medium (RPMI; Sigma) supplemented with 10% (v/v) heat-inactivated bovine calf serum (BCS; Hyclone), 1% (v/v) Penicillin-Streptomycin-Glutamine mixed solution (NACALAI TESQUE, INC.), 10mmol/L HEPES Buffer Solution (NACALAI TESQUE, INC.) and 1% (v/v) non-essential amino acids solution (NACALAI TESQUE, INC.). Tumor cell lines were kept at 37˚C in a humidified atmosphere of 95% air and 5% CO2 until use. Culture medium was replaced every 2 or 3 days.

Inoculation of tumor cell lines and evaluation of tumor growth

MC38/TfROVA-DTRs or 3LL-DTR were harvested and single-cell suspensions of 2×10^6 / 100 μL were intradermally inoculated into abdominal skin. For partial tumor cell death induction experiments, mixture of 1.4×10^6 of MC38/TfROVA-DTR cells and 0.6×10^6 of MC38 cells in 100 μL was intradermally inoculated into abdominal skin. Single-cell suspensions of 5×10^5 of B16-OVA or B16 in 100 μL were injected subcutaneously into the

flank. Tumor volumes were determined by caliper measurements and calculated using the formula: V=4⁄3*π*width/2*depth/2*height/2.

Photoconversion and surgical procedures

Tumor photoconversion was performed 5 days after tumor inoculation, as described previously (Nakanishi et al., 2017; Tomura et al., 2014). Briefly, KikGR mice were anesthetized with isoflurane (DS Pharma Animal Health) and luminal side of tumors was subjected to 120 seconds exposures to violet light (436 nm, 200 mW/cm^2) using SP500 spot UV curing equipment with a 436 nm bandpass filter (USHIO). During photoconversion, skin around tumors was protected from light with aluminum foil. After photoconversion, the abdominal wall was closed by suture. To keep exposed tissues moist during exposure to light, warmed phosphate buffered saline (PBS) was applied to region of photoconversion.

Cell isolation

Cell suspensions from tumors were prepared by enzymatic digestion. Tumors were finely dissected in RPMI 1640-medium (Sigma-Aldrich) containing 300 U/mL of collagenase from C.Histolyticum (Sigma-Aldrich), and 1 mg/mL of dispase II (Roche). After mincing with scissors, tumors were incubated in the same solution for 30 min at 37 ° C. After adding 2000 U/mL of DNase I (Calbiochem), cell suspensions were incubated for 15 min at 37 ° C, and filtered through a cell strainer. Preparation of cell suspensions from the LNs by enzymatic digestion was described previously (Tomura et al., 2014). Briefly, cell in LNs were extruded into RPMI 1640-medium containing 100 U/mL of collagenase type IV (Worthington) and 2000 U/mL of DNase I and incubated for 15 min at 37° C. After adding 0.5 M EDTA, cell suspensions were filtered through a cell strainer.

***In vitro* T cell proliferation assay**

Five days after tumor inoculation in KikGR mice, tumors were photoconverted. Twenty-four hours later, CD11c-positive cells in dLNs of tumor bearing KikGR mice were positively sorted using anti-CD11c magnetic microbeads (Miltenyi Biotec). Sorted cells were stained with Allophycocyanin (APC)-conjugated anti-mouse CD11c monoclonal antibody (mAb) and Alexa Fluor 700-conjugated anti-mouse I-A/I-E mAb, and KikGR-Red

and KikGR-Green cells in $CD11c^+$ MHC class II^{high} migratory DCs and KikGR-Green cells in $CD11c^{high}$ MHC class II^{int} LNDCs were sorted by SH800 (SONY). Mixture of LN and spleen cells from OT-I Tg mice were stained with biotinylated-CD4, CD11b, CD11c, CD19, CD49b, and TER-119 mAbs and negatively sorted using anti-biotin MACS beads (Miltenyi Biotec). Purity of $CD8^+$ TCR-$V\alpha2^+$ cells was >95 %. $CD8^+$ TCR-$V\alpha2^+$ cells (2×10^5 cells) were labeled with CellTrace Violet (Life Technologies) according to the manufacturer's protocol and co-cultured with sorted $CD11c^+$ MHC class II^{high} migratory KikGR-Red, KikGR-Green DCs or $CD11c^{high}$ MHC class II^{int} LNDCs (3×10^4 cells) for 72 hours in 96 well plate with in 2-Mercaptoethamnol containing RPMI-1640 medium. After three days of culture, cells were harvested and stained with PE/Cy7-conjugated anti-CD8 mAb, and APC-conjugated anti- TCR-$V\alpha2^+$ mAb and analyzed by flow cytometry. $CD8^+$ TCR-$V\alpha2^+$ T cell proliferation was evaluated by dilution of CellTrace Violet.

OT-I T-cell adoptive transfer and proliferation assay

Five days after tumor inoculation, mice were treated with DT and/or LPS, and twenty-four hours later, 1×10^6 of $CD8^+$ TCR-$V\alpha2^+$ CellTrace Violet labeled OT-I T cells were transferred intravenously. Forty-five hours after transfer, $CD8^+$ TCR-$V\alpha2^+$ T cell proliferation was evaluated by dilution of CellTrace Violet.

Microscopy and histology

Fluorescence images of tumors were captured with two-photon microscopy (A1, Nikon) or inverted microscope (ECULIPSE Ti-E, Nikon). For tumor imaging with inverted microscope, frozen sections of tumors were made. Five days after tumor inoculation, tumor bearing CD11c-YFP mice were treated with DT or vehicle and 24 hours later, tumors were dissected. After 24h fixation with 4% paraformaldehyde (Wako Chemicals), tumors were placed in 30% sucrose as a cryoprotectant. Frozen tissues were cut into 10 or 20 μm thick sections using a cryostat (CM1850, Leica) and observed with a fluorescence microscope.

Antibodies and Flow cytometry

Fluorochrome-conjugated or biotinylated mAbs and fluorochrome-conjugated avidin were obtained from BD Bioscience, eBioscience, Medical and Biological Laboratories co., ltd (MBL), Abcam or BioLegend. Details are listed in Supplementary Table 1. For flow cytometric analysis, cells were washed with Dulbecco's PBS containing 2% FCS and 0.02% sodium azide. Next, cells were incubated with 2.4G2 hybridoma culture supernatant to block Fc binding, then stained with biotinylated mAbs followed by Brilliant Violet 421-conjugated streptavidin or fluorochrome-labeled mAbs for 15 minutes at 4 ºC. For detection of OVA-specific TCR-bearing cells, cells were stained with phycoerythrin-conjugated H-2K^{b} OVA tetramer-SIINFEKL (MBL) for 30 minutes at room temperature (22-24 ºC) followed by staining with fluorochrome-labeled mAbs. Dead cells were labeled with Propidium Iodide (Wako) or 7-amino-actinomycin D just before flow cytometry analysis using SP6800 (SONY). Flow cytometry data were analyzed using FlowJo software (Tree Star). The number of cells per gram of tumor was calculated by dividing the number of cells obtained from flow cytometric analysis by the weight of the tumor used for the analysis. The number of cells in each cell subset in the lymph node was calculated by multiplying the total number of cells by the frequency of each cell subset obtained by flow cytometric analysis.

Reagents and treatment

One microgram of DT (Sigma-Aldrich) in PBS was injected intraperitoneally into tumor bearing mice 5 days after tumor inoculation. In some experiments, tumor bearing mice were intratumorally treated with 250 ng of LPS (Sigma-Aldrich) 5 days after tumor inoculation. Three hundred μg of oATP, 1 μg of A740003 (ChemScene), 50 μg of aHMGB1 mAb (Biolegend), 5 mg of glycyrrhizin dipotassium salt hydrate (Tokyo Chemical Industry), 100 μg of FTY720 (Cayman Chemical), or 500 ng of PTX (Wako) were injected intraperitoneally at the same time as DT treatment.

CRT expression assay

Single-cell suspensions of MC38/TfROVA-DTR cells (1.5×10^5 cells / 500 μL in serum-free media) were seeded into a 24-well dish and incubated for 3 hours, then 500 ng of DT was added. Eighteen hours later, cells were harvested and stained with anti-CRT mAbs and analyzed by flow cytometry.

HMGB1 and ATP release assay

Single-cell suspensions of MC38/TfROVA-DTR, 3LL-DTR or NIH/3T3-DTR cells (1.5×10^5 / 500 μL in serum-free media) were seeded into a 24-well dish and incubated for 3 hours, then 500 ng of DT was added. Twelve hours later, culture supernatants were harvested. HMGB1 and ATP concentrations in supernatants were measured by HMGB1 ELISA Kit (Arigo Biolaboratories Corp) and the luciferin-based ENLITEN ATP Assay (Promega, Madison, WI, USA), respectively.

Statistical analysis

Data were tested by Mann-Whitney's U test, one-way ANOVA with Holm-Sidak's multiple comparisons test, Kruskal-Wallis test with Dunn's comparisons test, two-way ANOVA with Sidak's multiple comparisons test, or Wilcoxon matched-pairs signed rank test, which were selected depending on the comparison group and data distribution. All tests were done using GraphPad Prism version 7.0 (GraphPad Software). Data in bar graphs represent means ± SEM. P-values of less than 0.05 were considered to be statistically significant and labeled: *, $P < 0.05$; **, $P < 0.01$; or ***, $P < 0.001$.

Supplemental References

Furukawa, N., Saito, M., Hakoshima, T., Kohno, K., 2006. A diphtheria toxin receptor deficient in epidermal growth factor-like biological activity. J. Biochem. 140, 831–841. https://doi.org/10.1093/jb/mvj216

Hogquist, K.A., Jameson, S.C., Heath, W.R., Howard, J.L., Bevan, M.J., Carbone, F.R., 1994. T cell receptor antagonist peptides induce positive selection. Cell 76, 17–27. https://doi.org/10.1016/0092-8674(94)90169-4

Kogure, T., Karasawa, S., Araki, T., Saito, K., Kinjo, M., Miyawaki, A., 2006. A fluorescent variant of a protein from the stony coral Montipora facilitates dual-color single-laser fluorescence cross-correlation spectroscopy. Nat. Biotechnol. 24, 577–581. https://doi.org/10.1038/nbt1207

Lindquist, R.L., Shakhar, G., Dudziak, D., Wardemann, H., Eisenreich, T., Dustin, M.L., Nussenzweig, M.C., 2004. Visualizing dendritic cell networks in vivo. Nat. Immunol. 5, 1243–1250. https://doi.org/10.1038/ni1139

Nakanishi, Y., Ikebuchi, R., Chtanova, T., Kusumoto, Y., Okuyama, H., Moriya, T., Honda, T., Kabashima, K., Watanabe, T., Sakai, Y., Tomura, M., 2017. Regulatory T cells with superior immunosuppressive capacity emigrate from the inflamed colon to draining lymph nodes. Mucosal Immunol. https://doi.org/10.1038/mi.2017.64

Saito, M., Iwawaki, T., Taya, C., Yonekawa, H., Noda, M., Inui, Y., Mekada, E., Kimata, Y., Tsuru, A., Kohno, K., 2001. Diphtheria toxin receptor-mediated conditional and targeted cell ablation in transgenic mice. Nat. Biotechnol. 19, 746–750. https://doi.org/10.1038/90795

Spiess, P.J., Yang, J.C., Rosenberg, S.A., 1987. In vivo antitumor activity of tumor-infiltrating lymphocytes expanded in recombinant interleukin-2. J. Natl. Cancer Inst. 79, 1067–1075.

Teasdale, R.D., D'Agostaro, G., Gleeson, P.A., 1992. The signal for golgi retention of bovine β1,4-galactosyltransferase is in the transmembrane domain. J. Biol. Chem. 267, 4084–4096.

Tomura, M., Hata, A., Matsuoka, S., Shand, F.H.W., Nakanishi, Y., Ikebuchi, R., Ueha, S., Tsutsui, H., Inaba, K., Matsushima, K., Miyawaki, A., Kabashima, K., Watanabe, T., Kanagawa, O., 2014. Tracking and quantification of dendritic cell migration and antigen trafficking between the skin and lymph nodes. Sci. Rep. 4, 1–11. https://doi.org/10.1038/srep06030

Yamazaki, C., Sugiyama, M., Ohta, T., Hemmi, H., Hamada, E., Sasaki, I., Fukuda, Y., Yano, T., Nobuoka, M., Hirashima, T., Iizuka, A., Sato, K., Tanaka, T., Hoshino, K., Kaisho, T., 2013. Critical Roles of a Dendritic Cell Subset Expressing a Chemokine Receptor, XCR1. J. Immunol. 190, 6071–6082. https://doi.org/10.4049/jimmunol.1202798